Defect evolution in Ni and solid-solution alloys of NiFe and NiFeCoCr under ion irradiation at 16 and 300 K

C. Mieszczynski[1], R. Ratajczak[1], J. Jagielski[1,2], G. Velişa[3], H. Bei[4], B.C. Sales[3], E. Wendler[5], W. J. Weber[4,3], Y. Zhang[3,4]

[1] *NOMATEN MAB+ Group*, National Centre for Nuclear Research, A. Soltana 7, 05-400 Otwock-Swierk, Poland

[2] Lukasiewicz - Institute of Electronic Materials Technology, Wolczynska 133, 01-919 Warsaw, Poland

[3] *Materials Science and Technology Division*, Oak Ridge National Laboratory, Tennessee 37831, USA

[4] *Department of Materials Science and Engineering*, University of Tennessee, Knoxville, TN 37996, USA

[5]*Institut für Festkörperphysik*, Friedrich-Schiller-Universität Jena, Jena, Germany

Abstract

Single-phase concentrated solid-solution alloys (SP-CSAs) have shown unique chemical complexity at the levels of electrons and atoms, and their defect evolution is expected to be different from conventional dilute alloys. Single crystals of Ni, NiFe and NiFeCoCr are chosen as model systems to understand the chemical complexity on defect formation and damage accumulation in SP-CSAs under ion irradiation. The high-quality crystals were irradiated at 16 and 300 K to different ion fluences, to form irradiated region with little to heavy damages. The ion-induced damage was determined using Rutherford backscattering spectrometry technique along a channeling direction (RBS/C) and the level of lattice damage in irradiated Ni and SP-CSAs was quantified from Monte Carlo (MC) simulations. The results are interpreted using the Multi Step Damage Accumulation model to reveal material damage accumulation kinetics. Key findings of the study are that in case of room temperature irradiations the damage level measured for complex alloys at the highest irradiation fluence of 2×10^{15} cm^{-2} (~3 dpa) is significantly higher than that obtained for pure nickel samples and suggest two-step damage accumulation process with a defect transformation taking place at a fluence of about 1.5×10^{15} cm^{-2}. Moreover, structural

and damage kinetic differences clearly imply that, with increasing degree of chemical complexity and high solid-solution strengthening effects from Ni to NiFe and to NiFeCoCr, the enhanced lattice stiffness resists to randomization of atomic configurations and inhibits the growth of extended defects.

Keywords: Single-phase concentrated solid-solution alloys, RBS/C, MC simulations, Ion-solid interactions, damage distribution

1. Introduction

One of the most important branches of chemical and nuclear industry is to understand and identify new materials resistant to specific operating conditions (e.g., irradiation, high temperature, corrosive environment). Because of specific operational conditions, parts of the structural components are exposed to damage due to radiation defects build-up in the materials. Obviously, the materials expected to be used in a radiative environment must fulfill severe safety requirements, the radiation resistance is of paramount importance. One of the most promising structural alloys, still in the testing phase regarding possible use in new generation of nuclear power plants (NPPs), are multi-component nickel superalloys [**1-3**].

In the presented paper radiation defects are created by ions having energy in hundreds of keV range, i.e. when elastic collisions are the dominant mechanism of energy losses. The ballistic nature of implantation processes leads to structural defects that are formed inside investigated materials. Significant advantages of ion irradiation include well-controlled concentration and depth distribution of defects, rapidly achievable high-level damage, and non-radioactive samples for easy handling [**4**]. The defect accumulation in materials is a complex process and usually has a multistage nature. The thresholds of subsequent structural transformations depend not only on the fluence of ions (hence dose of irradiation) [**5-7**], but also on the chemical composition of the investigated materials [**8-10**]. Single-phase concentrated solid-solution alloys (SP-CSAs) have shown unique properties at the levels of electrons and atoms [**2**,**3**,**11,12**] and their defect evolution is expected to be different from conventional dilute alloys. Single crystals of Ni, NiFe and NiFeCoCr are chosen as model systems, as they have increasing degree of chemical complexity [**2,12**], yield strength, lattice stiffness and toughness [**13**]. The main aim is therefore to compare damage build-up in several Ni-based alloys irradiated at various temperatures to get an insight into a role of alloy constituents on radiation resistance of the materials.

Rutherford backscattering spectrometry in a channeling direction (RBS/C) technique is widely used for quantitative analysis of damage level in ion implanted crystals. However, standard method of spectra deconvolution (so-called Two Beam Approximation – TBA [**14**]) which is typically used, suffers from several deficiencies. This is due to the fact, that TBA analysis assumes the existence of one type of defects only, so called Equivalent Scattering Centers (ECS), which may be regarded as a model of amorphous structure. In real situations in metals and alloys and many radiation-resistant ceramics mainly dislocations and dislocation loops are formed, which may lead in some cases (i.e., multi-component crystals, high-energy irradiation or presence of complex defects) to deceptive conclusions using TBA analysis. Therefore, in order to obtain reliable results assuming presence of dislocations in irradiated alloy (experimental data for 16 K have been presented before in Ref. 15) instead of using TBA model Monte Carlo based simulations using McChasy code was used (for a description of the code see Refs **16** and **17**). McChasy code reproduces RBS/C experimental spectra by simulating He-ions traveling inside the crystal structures and calculating the probability of the backscattering process. During the simulation processes, the code takes into account given defect distributions of randomly displaced atoms (RDA, alike to ECS) and extended defects (edge dislocation-bent channel). The possibility to differentiate between various types of defects provides a unique path forward to follow their evolution as a function of ion fluence and to study the role of chemical complexity on defect formation and damage accumulation in SP-CSAs under ion irradiation.

2. Experiment/Methods

Experiments were performed at two institutes; Friedrich Schiller University Jena (FSU, https://www.uni-jena.de/), Germany and Ion Beam Materials Laboratory (IBML, http://ibml.utk.edu/) in University of Tennessee Knoxville, USA [**18**]. The high-quality single crystals of pure Ni metal and two equiatomic NiFe and NiFeCoCr alloys were irradiated with 500 keV Ar^+ (FSU) and 550 keV Si^+ (IBML) ions with a wide range of fluencies ranging from 2×10^{13} up to 1×10^{16} cm^{-2} at both 16 K and room temperature (300 K), respectively. In both cases, the irradiation fluences were relatively low, and the possible influence of stoichiometry changes by incoming ions is negligible. The IBML irradiations were performed at relatively large incident angle of 30° in order to produce shallow damage, close to the 500 keV Ar^+ irradiation performed at FSU. The disorder in the irradiated samples was measured

by recording RBS/C spectra in the <100> aligned direction with 1.4 MeV He ions at FSU and 2.0 MeV in case of IBML experiments.

Experimentally obtained RBS/C spectra were simulated using Monte Carlo (MC) McChasy code developed at National Centre for Nuclear Research (NCBJ), Poland [**16**]. For comparison, the mean projected range of ions and induced defect distribution for Ar, as well as Si ions, were estimated from Stopping and Range of Ions in Matter (SRIM) simulations using the full cascade mode [**19,20,21**]. The ion distribution was estimated from the second column in RANGE.txt. The corresponding displacements per atom (dpa) profiles were predicted using two files, VACANCY.txt and NOVAC.txt under an assumed displacement energy threshold of 40 eV for all elements. For the full-cascade simulations, the dpa profile was the sum of the predicted vacancy concentrations using the column of "Knock-Ons" for Ar or Si ions and the columns of "Vacancies" from target elements (Ni vacancies and Fe vacancies in the case of NiFe) in VACANCY.txt, together with the replacement collisions in NOVAC.txt [**22**]. Note that ion-induced damage in both monoatomic and multi-elemental targets with a significant mass difference should be predicted using the full-cascade simulations [**20,21**], as the quick Transport of Ions in Matter (TRIM) option based on Kinchin-Pease holds only for monoatomic targets [**23**]. The SRIM estimated damage peaks are located at about 155 nm (Ar^+) and 190 nm (Si^+) for experiments performed at FSU and IBML, respectively.

The MC simulations were performed under the conditions that mimic the experiment (same geometry, backscattering angle, etc.), thermal vibrations of atoms were assumed to be in few pm range and the number of ions used in MC simulations was usually in few tens of thousands range to reach sufficiently good statistics.

The McChasy simulations were done on the basis of the extended defects representation. The McChasy model of extended defects is based on the Peierls-Nabarro model of an edge dislocations in which atoms are shifted from regular lattice positions following an arctan function with the bending angle decreasing asymptotically with the distance from dislocation core. For presented simulation the influence of distortions is cut above fifteen atomic rows. Detailed description about the simulation procedures and the Peierls-Nabarro model can be found elsewhere [**24**,**25**]. The solid lines present at the **Figure 1** are corresponding to spectra in aligned (001) direction obtained using MC simulations.

3. Results and discussion

3.1 Irradiations

The reason behind having two different irradiation temperatures (16 K and 300 K) was to study the temperature impact on microstructural changes occurring in Ni and SP-CSAs. While vacancies are not mobile at both temperatures, interstitials are believed to be immobile below temperatures of ~ 40 K. The experiment was aimed at a comparison between materials at room temperature with mobile interstitials and the one with immobile defects. Since more localized heat from slow dissipation of radiation energy is shown to enhance defect recombination [**12**], Ni, NiFe and NiFeCoCr are chosen as model systems based on the large difference in their thermal conductivity (κ_{Total}, see **Table 1**) [**2,18**], especially at low temperatures. As shown in **Table 1**, the lattice thermal conductivity (κ_{phonon}) is negligible in Ni, compared with the electrical thermal conductivity ($\kappa_{electron}$) at all temperatures. The low electrical resistivity (ρ_1 and ρ_2) and high thermal conductivity (κ_{Total}) of Ni suggest that radiation energy can be dissipated rapidly by electrons. The electrical resistivity for NiFe and NiFeCoCr at low temperatures is much higher than that in Ni, with slight increase for example from 10.3 to 11.0 $\mu\Omega$ cm and 77.1 to 78.4 $\mu\Omega$ cm at temperatures from 5 to 50 K, respectively, indicating less efficiency in heat conduction by electrons in the two alloys at low temperatures. While the lattice conductivities (κ_{phonon}) are similar for NiFe and NiFeCoCr at low temperatures (5 and 50 K), the dominate electrical thermal conductivities ($\kappa_{electron}$) have large differences, and the values of NiFe are ~ 7.5 times higher than those for NiFeCoCr. While NiFe is more conductive, such differences decrease at 300 K. Low-temperature experiments were performed to better reveal the defect dynamics resulting from the intrinsic electronic and atomic properties in SP-CSAs by minimizing thermal effects (e.g., less thermal vibrations of atoms at 16 K that is assumed to be in few pm range). At 300 K, lower damage saturation level is expected due to relatively increased mobility of atoms and more localized heat (associated to lower electrical conductivities), hence more efficient defect recombination/annihilation at room temperature or increased possibility to form larger defect clusters with increasing radiation dose. Under the sample irradiation dose, higher density of smaller clusters is expected to form under low temperature irradiations, which result in higher damage saturation level form the 16 K irradiations. On the basis of investigations performed, the trend in the evolution is determined by analyzing backscattering yield.

Table 1. The measured electrical resistivities (ρ_1 and ρ_2, $\mu\Omega$ cm) and total thermal conductivity (κ_{Total}, W/m K) of pure Ni, NiFe and NiFeCoCr [**2,18**] at 5, 50, 100 and 300 K The resistivity was measured twice, and the differences indicate the measurement error and difference in the alloys. The electrical thermal conductivities ($\kappa_{electron}$, W/m K) is estimated from the measured electrical resistivities and the Wiedemann–Franz relation. The resulting contribution of lattice conductivity ($\kappa_{phonon}=\kappa_{Total}-\kappa_{electron}$, W/m K) is listed in the last column.

T= 5 K	**ρ_1 ($\mu\Omega$ cm)**	**ρ_2 ($\mu\Omega$ cm)**	**κ_{Total} (W/m K)**	**$\kappa_{electron}$ (W/m K)**	**κ_{phonon} (W/m K)**
Ni	≈0.1	≈0.1	≈280	—	—
NiFe	10.3	10.0	1.67	1.18	0.49
NiFeCoCr	77.1	78	0.59	0.15	0.44
T= 50 K					
Ni	0.16	0.19	328	651	—
NiFe	11.0	10.6	15.4	11.4	4
NiFeCoCr	78.4	79	6.2	1.52	4.68
T= 100 K					
Ni	0.97	1.1	137	245	—
NiFe	13.4	12.8	22.5	19	3.4
NiFeCoCr	80.6	81.5	9.0	3	6
T= 300 K					
Ni	7.8	8.3	88	88	—
NiFe	36.5	35.0	28.0	21.1	7.6
NiFeCoCr	91.1	91.1	12.8	8.0	4.8

3.2 RBS/C analysis and simulations

Selected RBS/C spectra for NiFeCoCr alloys implanted with different fluences of Ar ions implanted at 16 K temperature are shown in **Figure 1(a)**. As a comparison in **Figure 1(b),** the spectra recorded for NiFeCoCr alloy implanted with Si ions at room temperature are presented. The RBS/C spectra and damage distributions for Ni and NiFe are shown as supplementary material [**26**].

As expected, the dechanneling level of aligned spectra increases as a function of Ar or Si fluence, following the damage induced inside the investigated material. It is worth pointing out that all investigated samples reveal similar damage behavior, regardless of ions used for creating defects. Either for low or high fluence, the apparent damage peak (starting next the surface peak, and centered at ~ 190 or 155 nm under Si^+ or Ar^+ ion irradiations, respectively) has not been formed. However, the dechanneling level increases significantly as a function of irradiation fluence. Such a result suggests that number of point defects or amorphous-like damage domains is limited, and mainly extended defects are formed inside investigated materials leading to the dechanneling of the analyzing beam. It is worth noting that the lowest energy configurations for interstitial-type defects in metals and alloys are dumbbell

interstitials [**27**] that cannot be treated as amorphous-like interstitials. These dumbbell interstitials are split pairs of atoms centered around one atomic position with a specific orientation. For example, the [100] dumbbells are reported as the most stable configuration in Ni-Fe alloys [**28**]. In other words, these dumbbell interstitials introduce local lattice strain (bending) and, if aligned with the ion beam, may lead to dechanneling of the He ions rather than direct backscattering of the channeled ions. Similar effect, namely bending of the atomic lines in the vicinity of the defects, can be observed near dislocation or dislocation loops. This is confirmed by the shape of the spectra, which do not reveal a formation of a clear damage peak near the end of range of irradiating ions but rather a continuous increase of the backscattering yield. This shape suggests that the backscattering is mainly due to the dechanneling of the analyzing beam, and not to a direct backscattering process on interstitial atoms. This behavior is indicative of the presence of dumbbell interstitials and/or dislocations in the irradiated material.

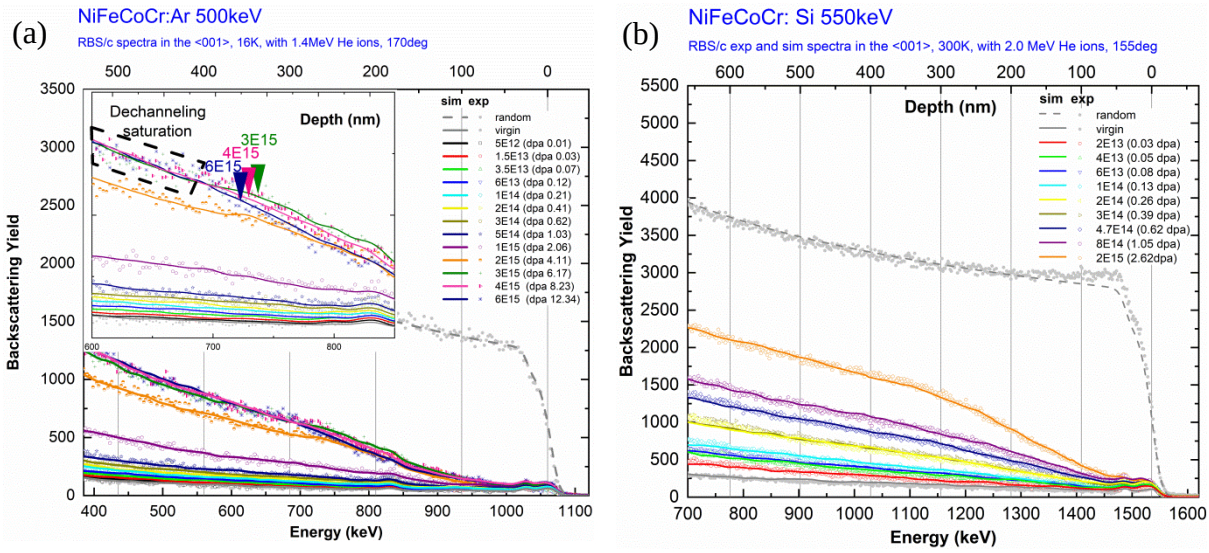

Figure 1. NiFeCoCr RBS/c spectra recorded along (001) direction. Comparison between NiFeCoCr implanted with Ar (a) and Si (b) ions. Solid lines represent fits obtained using MC simulations. Virgin and random spectra are included as references. An enlarged image is prepared as an inset to Fig. 1(a) to help observe the differences between the spectra.

The main important feature that should be noticed directly from the spectra is the saturation of damage level which is observed for the highest fluences (inset of **Fig. 1 (a)**).

Apart from the direct visible changes observed, the quantified information regarding damage induced in the material is revealed from damage distributions obtained from MC simulations. **Figure 2** is showing the results of the analysis performed using McChasy code. The

histograms show the quantitative values of the concentration of extended defects leading to dechanneling of the beam that were used to obtain the best fits of simulation curves to experimentally obtained data for SP CSA alloys.

The depths of simulated defect distributions are close to the SRIM predicted damage profiles (vacancies and ion distributions are plotted also with the damage distribution profiles at **Fig. 2**). To simplify comparison of damage for all measured materials, dpa values were calculated using the SRIM code.

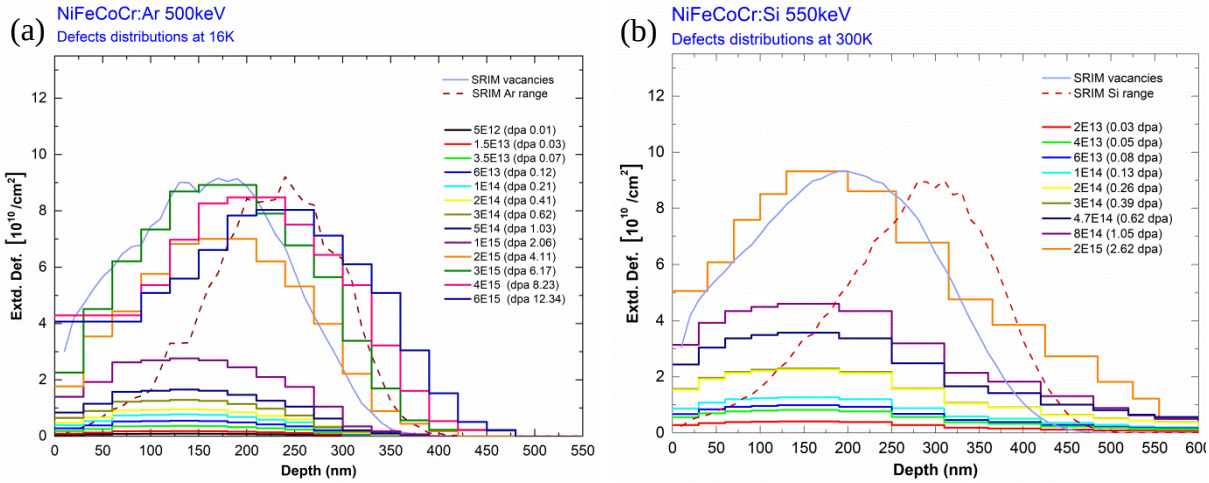

Figure 2. Damage distribution profiles obtained from MC simulations performed for RBS/C experimentally obtained spectra. SRIM predicted profiles of vacancies and ion ranges are also plotted. Total vacancies are used to calculate fluence related dpa values.

Quantitative results reveal similar, continuous dechanneling increase with the irradiation fluence for all investigated materials. All spectra have the shape characteristic for dominant presence of [100] dumbbell interstitials and/or dislocations: a continuous increase of the dechanneling yield with depth without formation of a clear damage peak.

3.3 Damage accumulation kinetics

In the majority of compound crystals structural transformations at specific fluencies occur, which can be visualized as steps in the defect accumulation curve. Therefore, the Multi-Step Damage Accumulation (MSDA) analysis was performed to reveal damage kinetics for investigated materials [**29,30**].

MSDA can be described as follows:

$$f_d = \sum_{i=1}^{n} (f_{d,i}^{sat} - f_{d,i-1}^{sat}) G[1 - \exp(-\sigma_i(\Phi - \Phi_{i-1}))] \quad (1)$$

where,

σ_i - cross-section for formation of a given kind of defect

$f_{d,\,i}^{sat}$ - level of damage at saturation for i-th kind of defects

Φ_i - fluence threshold for triggering the formation of i-th kind of defects

Figure 3 presents MSDA analysis performed for all investigated samples. Since [100] dumbbell interstitials are expected to be the most stable point defects, they do not cause direct backscattering of the channeled He ions, as would atoms in normal lattice interstitial sites. Consequently, in the following discussion, these dumbbell interstitials may be considered as defects leading to dechanneling of the analyzing beam. Points in the figure are corresponding to maximal values of extended defects formed in irradiated material. Solid lines are the fits made following MSDA equation (1).

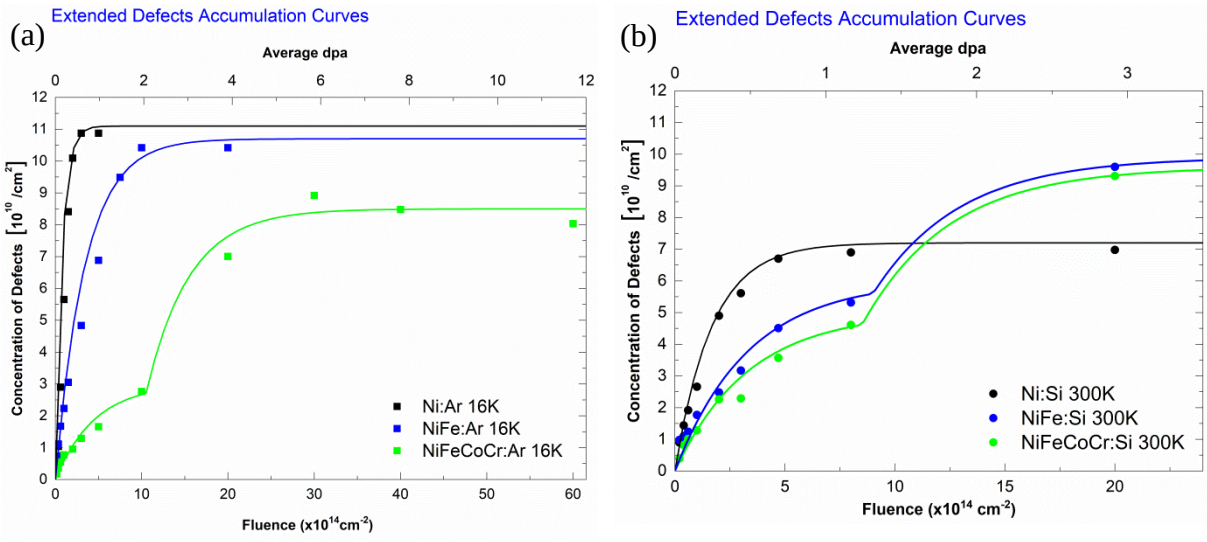

Figure 3. Damage kinetics for all investigated materials. Points represent the maximal values of extended defect distributions extracted from McChasy simulations, solid lines are fits to the experimental data using MSDA model.

The first clear outcome of the analysis is significantly lower level of saturation curves in samples irradiated at room temperature, when compared to low-temperature experiments. This is likely a logical effect of increased mobility of defects leading to more efficient annihilation. In case of low-temperature measurements, the cross-sections for damage

formation decreases for NiFe and NiFeCoCr alloys when compared to pure Ni material. (**Tab. 2**). the lower cross-section for damage formation observed for NiFe and NiFeCoCr alloys clearly suggests the suppression of defect growth. Similar situation can be observed for room temperature investigations. However, an increase in the number of formed defects in case of alloys may suggest kind of temperature effect for damage formation, for instance to more pronounced dislocation growth due to increased mobility of defects. It is worth mentioning that it is mainly due to the results obtained for last measured spectra (fluence equal to 2×10^{15} cm^{-2}) where we may observe rapid increase of the number of defects (clearly visible high increase of the dechanneling level observed in measured spectra). Numbers of extended defects formed for low irradiation fluences are well below values obtained for Ni (**Fig. 3 (b)**). However, at higher irradiation fluences one can observe more rapid increase of disorder level in complex alloys. This effect clearly suggests a transformation in a dominant defect structure, e.g. from dumbbells to dislocation loops or small loops and then to large loop transformation. In numerous irradiated materials this second step in damage accumulation kinetics was associated with transformation from small, few nm in size defects into dislocation loops and has been triggered by stress accumulation [31]. A higher number of smaller defect structures leads to a more pronounced lattice distortion in their vicinity, as compared to one large dislocation loop containing the same number of defects (likely in Ni or simple alloys), hence more efficient dechanneling of the analyzing beam (i.e., higher backscattering yield in RBS/c spectra).

Table 2. Cross-sections for defect formation extracted from the MSDA model

		$\sigma_1(10^{-14}cm^2)$	$fd_1(10^{10}\ cm^{-2})$	$\sigma_2(10^{-14}cm^2)$	$fd_2(10^{10}\ cm^{-2})$	$\Phi_2(10^{14}cm^{-2})$
16 K	**Ni:Ar**	1.3	11.1	-	-	-
	NiFe:Ar	0.3	10.7	-	-	-
	NiFeCoCr:Ar	0.2	3.0	0.2	8.5	10.5
300 K	**Ni:Si**	0.6	7.2	-	-	-
	NiFe:Si	0.3	5.0	0.25	9.6	8.5
	NiFeCoCr:Si	0.3	6.0	0.25	9.9	9.0

The results may suggest that there is a difference in defect migration and complex defect formation at room temperature between pure Ni and Ni-based alloys, as reported previously [**32**]. As reported elsewhere [**3,33,34**], additional extended defects may form as partial dislocations and/or faulted/unfaulted loops in SP CSAs with increasing irradiation fluence.

Such propositions are supported from transmission electron microscopy analysis of detailed defect structure in irradiated nickel and nickel-based alloys [**28, 32-35**].

4. Conclusions

The results obtained in this work can be summarized in the following statements. First of all, the analysis confirms the assumption that after irradiation mainly dumbbell interstitials with major crystal orientations, dislocations and/or dislocation loops are formed in SP-CSAs. The results presented were obtained using extended defects only (dislocations and well-aligned dumbbell interstitials) as a sole type of defects, this assumption has been suggested by shape of RBS/C spectra showing a continuous increase of the dechanneling yield with the increasing depth of analysis, the spectra do not contain typical damage peaks. Monte Carlo simulations of channeling spectra allows one to quantify the concentration of extended defects, such as dislocations and dumbbell interstitials aligned with the ion beam direction that do not cause direct backscattering of channeled ions, which is impossible using a standard TBA analysis. The results for 16 K show that the more complex structure of alloy is, the higher is its radiation resistance, i.e., the concentration of dislocations is lower than in pure nickel. The most resistant material is thus NiFeCoCr. The increase of the irradiation temperature leads to a decrease of concentration of dislocations too, very likely due to the increased mobility of defects. Moreover, an interesting observation has been found for Ni-based alloys. Pure Ni reveals single step accumulation kinetics (or very close to it), and may be reproduced by a simple Gibbons model. This behavior is typical for most of irradiated metals. NiFe and NiFeCoCr alloy irradiated at 300K, as well as NiFeCoCr irradiated at 16K, represent evident cases of a two-step damage accumulation kinetics, which can be interpreted as a change in dominant defect structure. Detailed, complex structural analysis is thus required to identify defects formed below and above 1×10^{15} cm^{-2} (or 2 dpa) to clarify this issue.

Acknowledgements

This work was supported as part of the Energy Dissipation to Defect Evolution (EDDE), an Energy Frontier Research Center funded by the U.S. Department of Energy, Office of Science, Basic Energy Sciences under contract number DE-AC05-00OR22725. Ion irradiations were performed at the Ion Beam Materials Laboratory (IBML, https://ibml.utk.edu/) located on the campus of the University of Tennessee, Knoxville. B.C.S.

was supported by the Department of Energy, Office of Science, Basic Energy Sciences, Materials Sciences and Engineering Division.

Data availability

The raw/processed data required to reproduce these findings cannot be shared at this time as the data also forms part of an ongoing study.

5. References

[1] J. H. Schneibel, *Beyond Nickel-Base Superalloys*, M. Gupta, T.S. Srivatsan, C.Y.H. Lim, R.A. Varin (Eds.), *Processing and Fabrication of Advanced Materials XIII*, vol. 2, Stallion Press, Singapore (2005) 563-574.
[2] Y Zhang, G. M. Stocks, K. Jin, Ch. Lu, H. Bei, B. C. Sales, L. Wang, Laurent K. Béland, R. E. Stoller, G. D. Samolyuk, M. Caro, A. Caro and W. J. Weber, *Influence of chemical disorder on energy dissipation and defect evolution in concentrated solid solution alloys*, Nature Commun., 6 (2015) 8736, https://doi.org/10.1038/ncomms9736.
[3] C. Lu, K. Jin, L. K. Béland, F. Zhang, T. Yang, L. Qiao, Y. Zhang, H. Bei, H. M. Christen, R. E. Stoller and L. Wang, *Direct Observation of Defect Range and Evolution in Ion Irradiated Single Crystalline Ni and Ni Binary Alloys*, Nature Sci. Rep. 6 (2016) 19994, https://doi.org/10.1038/srep19994.
[4] J.M. Poate and J .S. Williams, *Amorphization and Crystallization of Semiconductors in: Ion Implantation and Beam Processing*, J.M. Poate, Academic Press, Sydney 13 (1984), https://doi.org/10.1016/B978-0-12-756980-2.50005-9.
[5] Y. Zhang, I.-T. Bae, K. Sun, C. Wang, M. Ishimaru, Z. Zhu, W. Jiang, and W.J. Weber, *Damage Profile and Ion Distribution of Slow Heavy Ions in Compounds*, J. of Applied Physics 105 (2009) 104901, https://doi.org/10.1063/1.3118582.
[6] Y. Zhang, W. Jiang, C. Wang, F. Namavar, P.D. Edmondson, Z. Zhu, F. Gao, J. Lian, W.J. Weber, *Grain growth and phase stability of nanocrystalline cubic zirconia under ion* irradiation, Physical Review B 82 (2010) 184105, https://doi.org/10.1103/PhysRevB.82.184105.
[7] Y. Zhang, R. Sachan, O. H. Pakarinen, M. F. Chisholm, P. Liu, H. Xue, and W. J. Weber, *Ionization-induced annealing of pre-existing defects in silicon carbide*, Nat. Commun., 6 (2015) 8049, https://doi.org/10.1038/ncomms9049.
[8] R. Ratajczak, S. Prucnal, E. Guziewicz, C. Mieszczynski, D. Snigurenko, M. Stachowicz, W. Skorupa and A. Turos, *The photoluminescence response to structural changes of Yb implanted ZnO crystals subjected to non-equilibrium processing*, J. Appl. Phys. 121 (2017) 075101, https://doi.org/10.1063/1.4976207.
[9] R. Ratajczak, C. Mieszczynski, S. Prucnal, E. Guziewicz, M. Stachowicz, D. Snigurenko, J. Gaca, M. Wojcik, R. Böttger, R. Heller, W. Skorupa, J.V.Borany and A. Turos, *Structural and optical studies of Pr implanted ZnO films subjected to a long-time or ultra-fast thermal annealing*, Thin Solid Films 643 (2017) 24-30, https://doi.org/10.1016/j.tsf.2017.08.001.
[10] A. Turos, P. Jóźwik, M. Wójcik, J. Gaca, R. Ratajczak and A. Stonert, *Mechanism of damage buildup in ion bombarded ZnO*, Acta Materialia 134 (2017) 249-256, https://doi.org/10.1016/j.actamat.2017.06.005.

[11] Y. Zhang, S. Zhao, W. J. Weber, K. Nordlund, F. Granberg, and F. Durabekova, *Atomic-level heterogeneity and defect dynamics in concentrated solid-solution alloys*, Curr. Opin. Solid State Mater. Sci. 21 (2017) 221, https://doi.org/10.1016/j.cossms.2017.02.002.
[12] Y. Zhang, T. Egami, W.J. Weber, *Dissipation of radiation energy in concentrated solid-solution alloys: Unique defect properties and microstructural evolution*, MRS Bulletin 44 (2019) 798-811, https://doi.org/10.1557/mrs.2019.233.
[13] H.S. Oh, S.J. Kim, K. Odbadrakh, *et al., Engineering atomic-level complexity in high-entropy and complex concentrated alloys.*, Nat. Commun. 10 (2019) 2090, https://doi.org/10.1038/s41467-019-10012-7.
[14] E. Bøgh, *Defect studies in crystals by means of channeling*, Can. J. Phys. 46 (1968) 653-662, https://doi.org/10.1139/p68-081.
[15] G. Velişa, E. Wendler, S. Zhao, K. Jin, H. Bei, W.J.Weber, Y. Zhang, *Delayed damage accumulation by athermal suppression of defect production in concentrated solid solution alloys*, Mater. Res. Lett. 6 (2017) 136–141, https://doi.org/10.1080/21663831.2017.1410863.
[16] L. Nowicki, A. Turos, R. Ratajczak, A. Stonert, F. Garrido, *Modern analysis of ion channeling data by Monte Carlo simulations*, Nucl. Instr. Meth. Phys. Res. B 240 (2005) 277-282, https://doi.org/10.1016/j.nimb.2005.06.129.
[17] P. Jozwik, L. Nowicki, R. Ratajczak, A. Stonert, C. Mieszczynski, A. Turos, K. Morawiec, K. Lorenz, E. Alves, *Monte Carlo simulations for ion channeling analysis of damage in dislocation-containing crystals*, J. Appl. Phys. 126 (2019) 195107, https://doi.org/10.1063/1.5111619.
[18] Y. Zhang, M.L. Crespillo, H. Xue, K. Jin, C.-H. Chen, C.L. Fontana, J.T. Graham, and W.J. Weber, *New ion beam materials laboratory for materials modification and irradiation effects research*, Nucl. Instrum. & Meth. B 338 (2014) 19-30, https://doi.org/10.1016/j.nimb.2014.07.028.
[19] James F. Ziegler, M.D. Ziegler, J.P. Biersack, *SRIM-The stopping and range of ions in matter*, Nucl. Instr. Meth. Phys. Res. B 268 (2010) 1818-1823, https://doi.org/10.1016/j.nimb.2010.02.091.
[20] W.J. Weber and Y. Zhang, *Predicting Damage Production in Monoatomic and Multi-elemental Targets using Stopping and Range of Ions in Matter Code: Challenges and Recommendations*, Curr. Opin. Solid State Mater. Sci. 23 (2019) 100757, https://doi.org/10.1016/j.cossms.2019.06.001.
[21] J-P. Crocombette and Ch.Van Wambeke, *Quick calculation of damage for ion irradiation: implementation in Iradina and comparisons to SRIM*, EPJ Nucl. Sci. Tech. 5 (2019) 7, https://doi.org/10.1051/epjn/2019003.
[22] Y. Zhang, J. Lian, Z. Zhu, W.D. Bennett, L.V. Saraf, J.L. Rausch, C.A. Hendricks, R.C. Ewing, W.J. Weber, *Response of strontium titanate to ion and electron irradiation*, J. Nucl. Mater. 389 (2009) 303, https://doi.org/10.1016/j.jnucmat.2009.02.014.
[23] N. Andersen, P. Sigmund, K. Dan. Vidensk. Selsk., Mat.-Fys. Medd., 39 (1974) 1-45.
[24] P. Jóźwik, N. Sathish, L. Nowicki, J. Jagielski, A. Turos, L. Kovarik, B. Arey, S. Shutthanandan, W. Jiang, J. Dyczewski, A. Barcz, *Analysis of crystal lattice deformation by ion channeling*, Acta Phys. Pol. A 123 (2013) 828-830, https://doi.org/10.12693/APhysPolA.123.828.
[25] A. Turos, P. Jóźwik, L. Nowicki, N. Sathish, *Ion channeling study of defects in compound crystals using Monte Carlo simulations*, Nucl. Instr. Meth. Phys. Res. B 332 (2014) 50-55, https://doi.org/10.1016/j.nimb.2014.02.028.
[26] https://doi.org/10.17632/sbbmj83nsx.1
[27] S.C. Middleburgh, D.M. King, G.R. Lumpkin, M. Cortie, L. Edwards, *Segregation and migration of species in the CrCoFeNi high entropy alloy*, J. Alloys Compd. 599 (2014) 179–182, https://doi.org/10.1016/j.jallcom.2014.01.135.

[28] S. Zhao, Y. Osetsky, Y. Zhang, *Diffusion of point defects in ordered and disordered Ni-Fe alloys*, J. Alloys Compd., 805 (2019) 1175-1183, https://doi.org/10.1016/j.jallcom.2019.07.142.
[29] J. Jagielski and L. Thomé, *Multi-step damage accumulation in irradiated crystals*, Appl .Phys. A, 97 (2009) 147–155, https://doi.org/10.1007/s00339-009-5294-z.
[30] J. Jagielski, L. Thomé, A. Chartier, O. Dorosh, C. Mieszczynski, I. Jozwik, *Damage accumulation studies in ion-irradiated oxides: Current status and new perspectives*, Nucl. Instr. Meth. Phys. Res. B 435 (2018) 2-7, https://doi.org/10.1016/j.nimb.2017.11.015.
[31] J. Jagielski and L. Thomé, *Discontinuous character of the damage build-up in the elastic collision regime*, Rad. Eff. and Def. in Solids, 166 (2011) 367-372, https://doi.org/10.1080/10420150.2011.556117.
[32] D.S. Aidhy, Ch. Lu, K. Jin, H. Bei, Y. Zhang, L. Wang, W.J. Weber, *Point defect evolution in Ni, NiFe and NiCr alloys from atomistic simulations and irradiation experiments*, Acta Materialia 99 (2015) 69-76, https://doi.org/10.1016/j.actamat.2015.08.007.
[33] M.-R. He, S. Wang, S. Shi, K. Jin, H. Bei, K. Yasuda, S Matsumura, K. Higashida, I.M. Robertson, *Mechanisms of radiation-induced segregation in CrFeCoNi-based single-phase concentrated solid solution alloys*, Acta Materialia 126 (2017) 182-193, https://doi.org/10.1016/j.actamat.2016.12.046.
[34] C. Lu, T. Yang, K. Jin, N. Gao, P. Xiu, Y. Zhang, F. Gao, H. Bei, W.J. Weber, K. Sun, Y. Dong, L. Wang, *Radiation-induced segregation on defect clusters in single-phase concentrated solid-solution alloys*, Acta Materialia 127 (2017) 98-107, https://doi.org/10.1016/j.actamat.2017.01.019.
[35] S. Shi, M.-R. He, K. Jin, H. Bei, I.M. Robertson, *Evolution of ion damage at 773K in Ni-containing concentrated solid-solution alloys*, J. Nucl. Mater. 501 (2018) 132-142, https://doi.org/10.1016/j.jnucmat.2018.01.015.